Journal of Nuclear Medicine, published on December 20, 2019 as doi:10.2967/jnumed.119.234062

Quantitative 3D assessment of ^{68}Ga-DOTATOC PET/MRI with diffusion-weighted imaging to assess imaging markers for gastroendopancreatic neuroendocrine tumors: Preliminary results

Lisa C. Adams[1*], Keno K. Bressem[2*], Julia Brangsch[3], Carolin Reimann[4], Kristin Nowak[5], Winfried Brenner[6], Marcus R. Makowski[7]

[*]These authors contributed equally.

[1]Corresponding author. Department of Radiology and Nuclear Medicine, Charité, Charitéplatz 1, 10117 Berlin, Germany. Telephone number: +49 30 450 627 376. Fax number: +49 30 4507527911. Lisa.adams@charite.de. Resident.
[2]Department of Radiology and Nuclear Medicine, Charité, Charitéplatz 1, 10117 Berlin, Germany.
[3]Department of Radiology and Nuclear Medicine, Charité, Charitéplatz 1, 10117 Berlin, Germany.
[4]Department of Radiology and Nuclear Medicine, Charité, Charitéplatz 1, 10117 Berlin, Germany.
[5]Department of Radiology and Nuclear Medicine, Charité, Charitéplatz 1, 10117 Berlin, Germany.
[6]Department of Nuclear Medicine, Charité, Charitéplatz 1, 10117 Berlin, Germany.
[7]Department of Radiology and Nuclear Medicine, Charité, Charitéplatz 1, 10117 Berlin, Germany.

Running Title: PET/MRI with DWI to characterize GEP-NET

Word count: 4963

ABSTRACT

^{68}Ga-DOTATOC-PET/MRI (^{68}Gallium-DOTATOC-positron emission tomography/magnetic resonance imaging) combines the advantages of PET in the acquisition of metabolic-functional information with the high soft tissue contrast of MRI. Standardized uptake values (SUV) in tumors were suggested as a measure of somatostatin receptor expression. A challenge with receptor ligands is, that the distribution volume is confined to tissues with tracer-uptake, potentially limiting SUV quantification. In this study, different functional, three-dimensional (3D) SUV, apparent diffusion coefficient (ADC) parameters and arterial tumor enhancement were tested for the characterization of gastroendopancreatic neuroendocrine tumors (GEP-NET). **Methods:** For this single-center, cross-sectional study, 22 patients with 24 histologically confirmed GEP-NET lesions (15 men/7 women; median, 61 years, range, 43-81 years), who received hybrid ^{68}Ga-DOTA-PET/MRI examinations at 3T between January 2017 and July 2019 met eligibility criteria. SUVs, tumor-to-background ratios (TBR), the total functional tumor volume (TFTV), ADC_{mean} and ADC_{min} were measured based on volumes of interest (VOI) and examined with receiver operating characteristic analysis to determine cut-off values for differentiation between low and intermediate grade GEP-NET. Spearman's rank correlation coefficients were used to assess correlations between functional imaging parameters. **Results:** The ratio of PET-derived SUV_{mean} and diffusion-weighted imaging (DWI)-derived ADC_{min} was introduced as a combined variable to predict tumor grade, outperforming single predictors. Based on a threshold ratio of 0.03 to be exceeded, tumors could be classified as grade 2 with a sensitivity of 86% and specificity of 100%. SUV and functional ADC values as well as arterial contrast enhancement parameters showed non-significant and mostly negligible correlations. **Conclusions:** As receptor density and tumor cellularity appear to be independent, potentially complementary phenomena, the combined

PET/MRI ratio SUV_{mean}/ADC_{min} may be used as a novel biomarker, allowing to differentiate between grade 1 and 2 GEP-NET.

Key words: gastroendopancreatic neuroendocrine tumors, ^{68}Ga-DOTATOC PET/MRI, diffusion-weighted imaging, combined PET/MRI ratio, tumor grades.

INTRODUCTION

Gastroendopancreatic neuroendocrine tumors (GEP-NET) are a rare and heterogeneous group of tumors, originating from neuroendocrine cells of the gastrointestinal tract with a wide spectrum of clinical behavior (*1*).

According to the World Health Organization classification, neuroendocrine tumors are divided into grade 1 (≤ 2% Ki-67 index), grade 2 (3-20% Ki-67 index) and grade 3 tumors (>20% Ki-67 index), depending on their proliferative activity (*2*). 5-year survival rates for grade 1 tumors are estimated to be 89% compared to 70% for grade 2 and less than 57% for grade 3 tumors (*3*), making tumor grading a valuable tool for prognostic assessment. Non-invasive tumor grading in particular would be of clinical benefit, as it could reduce risks associated with biopsy and improve preoperative assessment.

Overexpression of somatostatin receptors in most GEP-NET creates a highly specific target for molecular imaging with ^{68}Ga-labeled somatostatin analogs (e.g. ^{68}Ga-DOTATATE and DOTATOC), but also enables the development of new therapeutic approaches (*4*). The introduction of hybrid PET/MRI (positron emission tomography/magnetic resonance imaging) allows for simultaneous multiparametric imaging, combining a superior soft-tissue contrast, high spatial resolution and functional imaging, such as diffusion-weighted imaging (DWI) or tumor contrast agent enhancement, with the possibility to assess the intensity/density of somatostatin receptor expression using the standardized uptake value (SUV) (*5,6*). A correlation between somatostatin receptor expression and SUV values was proposed in previous research, supporting a qualification of ^{68}Ga-labeled somatostatin analogs in the diagnostics of GEP-NET (*7*). Besides, PET/MRI with ^{68}Ga-labeled somatostatin analogs also showed potential for the prediction of survival and treatment response in neuroendocrine tumors (*8*). However, a challenge with receptor

ligands is, that the distribution volume is confined to tissues with tracer-uptake, potentially affecting SUV quantification.

DWI is an MR-based imaging technique, allowing to quantify the degree of water motion by calculation of the apparent diffusion coefficient (ADC). It is recognized as a functional sequence, reflecting tumor cell density, but low-b-value images also enable an accurate depiction of the anatomy (*9,10*). Previous studies found associations between the ADC and histopathological tumor features, reporting relationships with proliferation activity in several cancer types and thus showing a potential for predicting the grade of differentiation and prognosis (*11-13*).

In order to identify the most suitable metric for image-based characterization of GEP-NET, the present study investigates different receptor density-related and functional parameters. Although SUV and ADC measurements as well as tumor enhancement are already established in cancer imaging, it is still not clear, to what extent they can provide complementary information in the context of tumor differentiation/physiology and whether there is a correlation between such PET and MRI parameters.

The aims of the present study were therefore *1)* to compare three-dimensional (3D) SUV and ADC parameters, such as SUV_{mean}, SUV_{max}, tumor-to-background ratio (TBR), ADC_{mean}, ADC_{min} and the total functional tumor volume TFTV, as well as arterial tumor enhancement across different GEP-NET grades, evaluating if they could identify the grade of differentiation with reliable diagnostic accuracy and *2)* to examine a potential association between functional 3D SUV and ADV values as well as arterial tumor enhancement to determine if they were correlated or independent.

MATERIALS AND METHODS

Patient population

Within this cross-sectional study, we prospectively acquired and analyzed 98 ^{68}Ga-DOTATOC-PET/MRI examinations for diagnostic evaluation of GEP-NET performed at our department between January 2017 and July 2019 (refer to Figure 1). The study was approved by the Institutional Review Board (EA1/060/16) and prior to the examinations all subjects signed a written informed consent.

Out of this consecutive cohort, 22 patients (7 women, 15 men; median, 61 years, age range, 43-81 years) with 24 primary or recurrent neuroendocrine tumors met the eligibility criteria (patient older than 18 years, gadolinium-enhanced ^{68}Ga-DOTATOC-PET/MRI as the index test, presence of a neuroendocrine tumor lesion in the gastrointestinal tract - as defined by ^{68}Ga-DOTATOC tracer uptake and/or contrast enhancement, no ongoing systemic therapy). 1 patient with a grade 3 GET-NET of the pancreas was excluded from analysis due to n=1 not being representative. Table 1 provides an overview of patient/tumor characteristics.

In all patients, the diagnosis of neuroendocrine tumor was histologically confirmed, so histopathological results served as the reference standard for this study. GEP-NET were classified into 3 grades according to the World Health Organization classification system by integrating the Ki-67 labeling index, and the presence of necrosis. Ki-67 labeling index was available in all but one patient.

Hybrid PET/MRI – Imaging protocol

Simultaneous PET/MRI was performed with a 3T MRI/PET Magnetom Biograph mMR hybrid system (Siemens Healthcare, Erlangen, Germany; software vB20P), featuring avalanche

photodiode and total imaging matrix coil technology. MR parameters included: MQ- Gradients: 45 mT/m maximum gradient amplitude; 200 T/m/s maximum gradient slew rate; LSO crystal; 4.3 mm transverse spatial resolution at FWHM at 1 cm; 15.0 kcps/MBq sensitivity at center; 13.8 kcps/MBq at 10 cm off-center.

The PET scan started 60 minutes after injection of ^{68}Ga-DOTATOC (mean activity, 160 MBq), comprising a whole-body-scan with 5 bed positions, each being 3 minutes long (30% overlap), from the skull base to the upper thigh with subsequent iterative HD PET image reconstruction (3 iterations), based on a x-matrix acquisition with a 4 mm Gaussian filter and relative scatter scaling. No adverse effects were observed after the injection of ^{68}Ga-DOTATOC. The pre-contrast MRI sequences were acquired simultaneously with a dedicated mMR head-and-neck coil and phased-array mMR body surface coils.

Table 2 provides an overview of MRI sequence and tabulated parameters. Gadolinium-based contrast administration was applied at a dose of 0.1 mL/kg body weight. The delay, as obtained by bolus tracking, was approximately 18 seconds for the arterial bolus

The total imaging time for the PET/MR study, including contrast-enhanced MRI, was 90 minutes. Post-acquisition data analysis was performed with syngo.MR General Engine (Siemens Healthcare).

Hybrid PET/MRI – Volumetric imaging analysis

All imaging datasets were evaluated on a Picture Archiving and Communication System workstation, using Visage (Visage 7.1, Visage Imaging, Berlin). One experienced radiologist analyzed fused gadobutrol-enhanced ^{68}Ga-DOTATOC-PET/MRI and native ^{68}Ga-DOTATOC-PET/DWI, identifying NET-positive lesions. On ^{68}Ga-enhanced PET/MRI images, focal ^{68}Ga-

accumulations with any kind of morphological correlate in a contrast enhanced or DWI series were regarded as NET-positive. Any discrepancies were resolved based on a separate consensus reading. The radiologists were blinded to the patient's identity and results of previous or follow-up imaging as well as histopathology/tumor grade. In order to avoid recognition bias, contrast enhanced ^{68}Ga-DOTATOC-PET/MRI and native ^{68}Ga-DOTATOC-PET/DWI were assessed in different sessions and random order, separated by a two-week period.

For segmentation, PET/MRI images were exported from the PACS as DICOM data and segmented with MITK (*14*). To analyze the functional volume, a semi-automatically delineated volume-of-interest (3D-VOI) was obtained in the respective lesion on the PET images, with an isocontour set to 70% of maximum uptake.

Quantitative analysis of ADC parameters was based on the high b-value images, where the NET was best visualized, incorporating voxels across multiple slices, and then, the VOI were copied to the ADC maps. Accordingly, quantitative values within the measured VOI were ADC_{mean} and ADC_{min}, determining the mean and minimum value of all voxels. The TFTV was obtained based on an isocontour of 70% and SUV_{mean} and SUV_{max} were measured within the corresponding 3D-VOI. The normalized quantitative tumor-to-background ratio (TBR) was calculated based on the background signal of the healthy tissue adjacent to the lesion.

Lesion/parenchyma contrast-to-noise-ratios (CNRs) were defined as the signal intensity of the lesion (SI lesion) minus SI parenchyma divided by the standard deviation of the background noise. The enhancement ratio of the respective lesion before and after the administration of gadolinium was calculated based on the following formula:

Enhancement ratio = (contrast-enhanced SI lesion – native SI lesion)/ native SI lesion

Statistical analysis

All statistical analysis was performed using the 'R' statistical environment (version 3.4.4). Values were expressed as means and standard deviations, if normally distributed and as median and interquartile range if not. For most non-normal distributed lesions, normalization could be achieved through logarithmic transformation. To assess the direction and strength of correlation between two variables, Spearman's correlation coefficients were calculated. Interpretation was as follows: a positive or a negative correlation coefficient of 0.90–1.00 was considered very high; 0.70–0.89, high; 0.40–0.69, moderate; 0.30–0.49, low; and 0–0.29, negligible (*15*). Boxplots were used to display the value distribution amongst different tumor grades, then a receiver operating characteristic analysis was performed to establish a cutoff for differentiation between grade 1 and grad 2 tumors. Significance levels are indicated as $p < 0.05$, $p < 0.01$, $p < 0.001$, and $p < 0.0001$.

RESULTS

There were 12 grade 1 tumors (48.0%) and 12 grade 2 tumors (48.0%). The mean maximum diameter, as measured on axial MRI was 29.6 mm ± 23.8 mm (range 11 to 95 mm) and the mean TFTV was 36.8 cm^3 ± 82.0 cm^3 (range 1.1 cm^3 to 351.1 cm^3) (also refer to Table 1).

Comparison of histologic grades with tumor size, enhancement, SUV and ADC parameters and tumor volume (preliminary data)

Grade 2 tumors were significantly larger than grade 1 tumors (40.7 mm ± 30.4 mm (range 11.0 mm to 40.0 mm) versus 19.7 mm ± 9.6 mm (range 12.0 mm to 95.0 mm), $p<0.05$). The TFTV was higher in grade 2 tumors compared to grade 1 tumors (70.6 cm^3 ± 112.2 cm^3 (range 1.5 cm^3 to 351.1 cm^3) versus 6.4 cm^3 ± 9.9 cm^3 (range 1.2 cm^3 to 34.2 cm^3), p=0.06)). Among SUV parameters, SUV_{mean} (measured within a 3D-VOI) was significantly higher in grade 2 tumors compared to grade 1 tumors (23.1±12.3 (range 8.0-45.0) versus 14.7±7.0 (range 4.0-23.2), $p<0.05$). SUV_{max} was also higher in grade 2 tumors compared to grade 1 tumors (42.3 ± 26.6 (range 14.8-89.5) versus 34.9 ± 16.9 (range 14.5-62.5); however, this difference was not significant, p = 0.25). Normalized TBR values were also higher in grade 2 tumors compared to grade 1 lesions (12.7±9.3 (range 3.9 to 33.2) versus 6.6±1.9 (range 3.1 to 10.1), $p<0.05$). Regarding ADC parameters measured, grade 2 tumors showed significantly lower ADC_{mean} values than grade 1 tumors (960.7±262.2 (range 500 to 1221) versus 1235.9±183.0 (range 1045 to 1486), $p<0.05$). ADC_{min} values were also lower in grade 2 tumors compared to grade 1 tumors; however, these differences were not significant (492.9±244.0 (range 225.5 to 849.5) versus 665.2±135.5 (range 510.5 to 868.5), p=0.17). Regarding the evaluation of arterial contrast enhancement, enhancement ratios were marginally higher for grade 1 GEP-NET compared to grade 2 GEP-NET (1.2±0.8

(range 0.6 to 2.9) versus 1.0±0.4 (range 0.4 to 1.6), p=0.5). Refer to Table 3 for tabulated lesion characteristics.

Comparing Ki-67 labelling index to tumor size, tumor volume, SUV and ADC parameters (preliminary data)

Correlation analyses between the quantitative 3D imaging parameters and the Ki-67 labelling index were performed for 22 patients (not available in one patient). TFTV showed a positive correlation with Ki-67 ($r=0.65$, $p<0.05$), while ADC_{mean} showed a weaker correlation ($r=-0.37$, $p=0.07$). Otherwise none of the imaging values measured within 3D-VOI correlated at least moderately with Ki-67. Figures 2 and 3 and Supplemental Figures 1 and 2 show exemplary images for one grade 1 and three different size 2 GEP-NET.

Logistic regression and receiver operating characteristic analysis

To identify cut-off values for SUV_{mean}, SUV_{max}, TBR, TFTV, ADC_{mean} and ADC_{min} to differentiate grade 1 and 2 tumors, receiver operating characteristic analyses were performed. Sensitivity and specificity (1- false positive rate) were calculated with varying cut-offs for all before-mentioned variables. The optimal cut-off-values were chosen based on the maximum sum of sensitivity and specificity. For SUV_{mean}, the cut-off value was 28, which means, that 2 tumors could be identified with a sensitivity of 44% and specificity of 100%, in case the SUV_{mean} values exceeded the cut-off value. For SUV_{max}, the cut-off value was 67, which means, that 2 tumors could be identified with a sensitivity of 22% and specificity of 100%, in case the SUV_{mean} values exceeded the cut-off value. For TBR, the cut-off value for 2 tumors to be exceeded was 12, yielding a sensitivity of 56% and a specificity of 100%; and for TFTV, the cut-off value to be exceeded

was 15.5, resulting in a sensitivity/specificity of 67% and 90%, respectively For ADC_{mean}, the receiver operating characteristic analysis suggested a cut-off of $1.06*10^{-3}$ mm^2/s, whereby tumors with values less than the cut-off value would be graded as 2 (sensitivity=67%, specificity=86%). For ADC_{min}, the receiver operating characteristic analysis suggested a cut-off of $0.50*10^{-3}$ mm^2/s, whereby tumors with values less than the cut-off value would be graded as 2 with a sensitivity=67% and a specificity of 100%. For differentiation between grade 1 and 2 tumors, SUV_{mean} was superior to SUV_{max} and ADC_{min} was superior to ADC_{mean}, respectively. However, as none of the single predictors provided optimal diagnostic accuracy, the ratio of SUV_{mean} and ADC_{min} was introduced as a combined variable to predict tumor grade, outperforming the single predictors for discrimination between grade 1 and grade 2 tumors. Based on a threshold ratio of 0.03 to be exceeded, tumors could be classified as grade 2 with a sensitivity of 86% and specificity of 100% (refer to Figure 4 for receiver operating characteristic analyses). Refer to Figures 2 and 3 for case examples of patients with low and intermediate grade GEP-NET.

Preliminary results on the association between 3D SUV and ADC values and arterial enhancement

The SUV and ADC values showed non-significant and negligible correlations (ADC_{min} and SUV_{max}, r=0.26, p=0.39; ADC_{mean} and SUV_{mean}, r=0.01, p=0.98; ADC_{min} and SUV_{mean}, r=0.15, p=0.62; ADC_{mean} and SUV_{max}, r=-0.05, p=0.88), suggesting an independency of the SUV- and ADC-based values, which would also be expected from a functional point of view.

Regarding a potential correlation between SUV values and contrast enhancement parameters, SUV_{max} and enhancement ratio or SUV_{max} and CNR_{art} showed moderate correlations of r=0.67 or r=0.53, which, did not reach significance levels (p=0.13 or p=0.06). All other

correlations were not significant and negligible (SUV_{mean} and CNR_{art}, r=0.44, p=0.14; SUV_{mean} and enhancement ratio, r=0.2, p=0.52). Supplemental Figure 3 demonstrates the scatterplots of the correlations between the examined correlations of the SUV and ADC parameters and between SUV and MRI enhancement values.

DISCUSSION

PET imaging plays a pivotal role in the diagnosis of GEP-NET. Our results suggest, that a combined assessment of the complementary parameters 3D SUV_{mean} and ADC_{min} allows for a reliable differentiation between low and intermediate grade GEP-NET. While 3D SUV_{mean} values were significantly higher, ADC_{min} was significantly lower in grade 2 tumors compared to grade 1 tumors. As to be expected considering the underlying functional mechanisms, the present study showed non-significant and mostly negligible correlation between ADC and SUV parameters and between ADC and contrast enhancement parameters.

The SUV is the most studied semiquantitative parameter in the analysis of tracer uptake in PET imaging and was suggested as a marker for the quantification of somatostatin receptor density in neuroendocrine tumors (*7,16*). While, so far, data on PET somatostatin receptor studies are limited, some studies suggested, that changes in tumor SUV did not reliably correlate with treatment outcome and the net uptake rate (Ki) (*17,18*). Accordingly, SUV may not offer a perfect reflection of somatostatin receptor expression.

Even though it appears difficult to establish a link between tracer avidity and histopathological tumor grade, it was previously demonstrated, that well-differentiated neuroendocrine tumors (grade 1 and 2 tumors) showed higher SUVs for ^{68}Ga-labeled somatostatin analogs compared to poorly differentiated neuroendocrine tumors (*19*). We found a significant difference between low and intermediate grade GEP-NET, with intermediate grade GEP-NET showing a higher ^{68}Ga-DOTATOC uptake, which is in contrast to previously published literature (*19*). We also found SUV_{mean} to be a more reliable predictor than SUV_{max}. But even when using SUV_{mean} as a single predictor for histopathological grade, only a poor to moderate diagnostic

accuracy could be achieved, suggesting, that SUV alone cannot be used for assessment of tumor grade.

Therefore, a complementary approach including SUV_{mean} and ADC_{min} was applied. DWI-based ADC values are based on a measure of cellularity. Since tumor cellularity is contributed largely by cellular proliferation, the ADC value can be considered a surrogate biomarker for tumor-cell proliferation. It may be assumed, that malignancies with a high proliferative index have higher cellularity and more restricted diffusion, resulting in lower ADC values. Previously, DWI ADC values demonstrated a potential to distinguish grade 1 from grade 2 and 3 neuroendocrine lesions and were also correlated with the Ki67-index (*20,21*). In line with this, we also identified ADC parameters, especially ADC_{min}, as potential predictors to differentiate between grade 1 and grade 2 GEP-NETs. Avoiding possible gadolinium-associated risks and as an alternative in case of contraindications for contrast agents, DWI could furthermore represent a cost-effective alternative to contrast-enhanced MRI for fused ^{68}Ga-DOTA-PET/MRI.

Regarding a potential relationship between SUV and ADC parameters, no correlation could be found, which was to be expected from a functional point of view, considering that ^{68}Ga-DOTATOC-based SUV is measure of receptor expression/density, while ADC is a surrogate marker of cellularity and restricted water diffusion. This is also line with previous research, where ADC and SUV values showed no correlations, irrespective of the underlying histological subtype, supporting their independency (*16,22*). It can be assumed, that SUV and ADC values illuminate different aspects of pathophysiology. A combination of PET-based receptor imaging with functional MRI information therefore provides complementary information with respect to tumor characterization. We incorporated 3D SUV and ADC parameters into one prediction model, which enabled a reliable differentiation between low and intermediate grade GEP-NET.

Since neuroendocrine tumors and their metastases are typically hypervascular, they often show arterial hyperperfusion (*23*). In the present study, we found large variations regarding this characteristic, which was particularly due to heterogeneous larger tumors, involving non-enhancing cystic, necrotic or hemorrhagic areas as well as hyperenhancing regions. In line with our findings, *Jeon et al.* reported hyperenhancement to be present in only approximately half of the cases, with otherwise iso- or hypoenhancement on arterial phase images (*24*). Regarding a potential association between functional ^{68}Ga-DOTATOC-PET/DWI SUV_{max} values and arterial enhancement patterns, measured by semi-quantitative CNR values, we could identify only moderate, nonsignificant correlations for SUV_{max} and the enhancement ratio or CNR_{art}.

There are limitations to the present study: Factors which could potentially influence the generalizability of the results include the hardware characteristics (i.e. different PET/MRI systems), the chosen imaging parameters, and the applied delineation technique. A main limitation of the present study is its small patient cohort, especially regarding intestinal NET lesions, which may have resulted in type 2 errors. On the other hand, GEP-NET are a relatively rare entity, while PET/MRI is novel technique. As there was only 1 grade 3 GEP-NET, this case was excluded and our analysis was limited to grades 1 and 2 GEP-NET. In addition, regarding the calculation of separate detection rates for contrast-enhanced MRI, DWI/MRI and PET/MRI there is an obvious selection bias. Finally, the premise, that PET/MRI-based assessment of gastroendopancreatic neuroendocrine tumors shows the potential to reduce or even alleviate the need for biopsy in the future might be premature. Further validation with larger patient populations will be required, specifically including grade 3.

CONCLUSION

As receptor expression and tumor cellularity appear to be independent phenomena, the combined PET/MRI ratio SUV_{mean}/ADC_{min}, which is based on 3D measurements of all voxels within the respective lesion volumes, may be used as a novel biomarker, allowing to differentiate between grade 1 and grade 2 GEP-NET. Therefore, multiparametric analysis from hybrid PET and DWI imaging might offer the potential to non-invasively acquire complimentary, image-based information on the proliferative activity of GEP-NET.

DECLARATION

List of abbreviations

3D	Three-dimensional
ADC	Apparent diffusion coefficient
CNR	Contrast-to-noise ratio
DWI	Diffusion-weighted imaging
Ga	Gallium
GEP-NET	Gastroendopancreatic neuroendocrine tumors
PET/MRI	Positron emission tomography/magnetic resonance imaging
ROI	Region of interest
SI	Signal intensity
SUV	Standardized uptake value
TFTV	Total functional tumor volume
TBR	Tumor-to-background ratio
VOI	Volume of interest

Financial disclosure

The authors have nothing to disclose.

Competing interests

None

Acknowledgements

MRM is grateful for support from the Deutsche Forschungsgemeinschaft (DFG, SFB 1340/1 2018, 5943/31/41/91). LCA is grateful for her participation in the BIH Charité - Clinician Scientist Program funded by the Charité - Universitaetsmedizin Berlin and the Berlin Institute of Health.

KEY POINTS

Question:

The purpose of this study was to compare and evaluate the use of the combined PET/MRI ratio SUV_{mean}/ADC_{min} as a biomarker for differentiation between low and intermediate grade primary or recurrent GEP-NET. Besides, a potential association between functional 3D SUV and ADV values as well as arterial tumor enhancement was investigated to determine if these parameters were correlated or independent.

Pertinent findings:

As receptor density and tumor cellularity appear to be independent, potentially complementary phenomena, the combined PET/MRI ratio SUV_{mean}/ADC_{min} may be used as a biomarker, allowing to differentiate between low and intermediate grade GEP-NET.

Implications for patient care:

Multiparametric analysis from hybrid PET and DWI imaging might offer the potential to non-invasively acquire complimentary, image-based information on the proliferative activity of GEP-NET, providing incremental diagnostic value beyond anatomical imaging.

REFERENCES

1. Diez M, Teule A, Salazar R. Gastroenteropancreatic neuroendocrine tumors: diagnosis and treatment. *Ann Gastroenterol.* 2013;26:29-36.

2. Saeger W, Schnabel PA, Komminoth P. [Grading of neuroendocrine tumors]. *Pathologe.* 2016;37:304-313.

3. Richards-Taylor S, Ewings SM, Jaynes E, et al. The assessment of Ki-67 as a prognostic marker in neuroendocrine tumours: a systematic review and meta-analysis. *J Clin Pathol.* 2016;69:612-618.

4. Haug AR, Cindea-Drimus R, Auernhammer CJ, et al. The role of 68Ga-DOTATATE PET/CT in suspected neuroendocrine tumors. *J Nucl Med.* 2012;53:1686-1692.

5. Paidpally V, Chirindel A, Lam S, Agrawal N, Quon H, Subramaniam RM. FDG-PET/CT imaging biomarkers in head and neck squamous cell carcinoma. *Imaging Med.* 2012;4:633-647.

6. Koukouraki S, Strauss LG, Georgoulias V, et al. Evaluation of the pharmacokinetics of 68Ga-DOTATOC in patients with metastatic neuroendocrine tumours scheduled for 90Y-DOTATOC therapy. *Eur J Nucl Med Mol Imaging.* 2006;33:460-466.

7. Kaemmerer D, Peter L, Lupp A, et al. Molecular imaging with (6)(8)Ga-SSTR PET/CT and correlation to immunohistochemistry of somatostatin receptors in neuroendocrine tumours. *Eur J Nucl Med Mol Imaging.* 2011;38:1659-1668.

8. Kaewput C, Suppiah S, Vinjamuri S. Correlation between standardized uptake value of (68)Ga-DOTANOC positron emission tomography/computed tomography and pathological classification of neuroendocrine tumors. *World J Nucl Med.* 2018;17:34-40.

9. Taouli B, Koh DM. Diffusion-weighted MR imaging of the liver. *Radiology.* 2010;254:47-66.

10. Zech CJ, Herrmann KA, Dietrich O, Horger W, Reiser MF, Schoenberg SO. Black-blood diffusion-weighted EPI acquisition of the liver with parallel imaging: comparison with a standard T2-weighted sequence for detection of focal liver lesions. *Invest Radiol.* 2008;43:261-266.

11. Surov A, Meyer HJ, Wienke A. Associations between apparent diffusion coefficient (ADC) and KI 67 in different tumors: a meta-analysis. Part 2: ADCmin. *Oncotarget.* 2018;9:8675-8680.

12. Sasaki T, Kim J, Moritani T, et al. Roles of the apparent diffusion coefficient and tumor volume in predicting tumor grade in patients with choroid plexus tumors. *Neuroradiology.* 2018;60:479-486.

13. Higano S, Yun X, Kumabe T, et al. Malignant astrocytic tumors: clinical importance of apparent diffusion coefficient in prediction of grade and prognosis. *Radiology.* 2006;241:839-846.

14. Wolf I, Vetter M, Wegner I, et al. The medical imaging interaction toolkit. *Med Image Anal.* 2005;9:594-604.

15. Mukaka MM. Statistics corner: A guide to appropriate use of correlation coefficient in medical research. *Malawi Med J.* 2012;24:69-71.

16. Fruehwald-Pallamar J, Czerny C, Mayerhoefer ME, et al. Functional imaging in head and neck squamous cell carcinoma: correlation of PET/CT and diffusion-weighted imaging at 3 Tesla. *Eur J Nucl Med Mol Imaging.* 2011;38:1009-1019.

17. Velikyan I, Sundin A, Sorensen J, et al. Quantitative and qualitative intrapatient comparison of 68Ga-DOTATOC and 68Ga-DOTATATE: net uptake rate for accurate quantification. *J Nucl Med.* 2014;55:204-210.

18. Kratochwil C, Stefanova M, Mavriopoulou E, et al. SUV of [68Ga]DOTATOC-PET/CT predicts response probability of PRRT in neuroendocrine tumors. *Mol Imaging Biol.* 2015;17:313-318.

19. Kayani I, Bomanji JB, Groves A, et al. Functional imaging of neuroendocrine tumors with combined PET/CT using 68Ga-DOTATATE (DOTA-DPhe1,Tyr3-octreotate) and 18F-FDG. *Cancer.* 2008;112:2447-2455.

20. Jang KM, Kim SH, Lee SJ, Choi D. The value of gadoxetic acid-enhanced and diffusion-weighted MRI for prediction of grading of pancreatic neuroendocrine tumors. *Acta Radiol.* 2014;55:140-148.

21. Wang Y, Chen ZE, Yaghmai V, et al. Diffusion-weighted MR imaging in pancreatic endocrine tumors correlated with histopathologic characteristics. *J Magn Reson Imaging.* 2011;33:1071-1079.

22. Goense L, Heethuis SE, van Rossum PSN, et al. Correlation between functional imaging markers derived from diffusion-weighted MRI and 18F-FDG PET/CT in esophageal cancer. *Nucl Med Commun.* 2018;39:60-67.

23. Worhunsky DJ, Krampitz GW, Poullos PD, et al. Pancreatic neuroendocrine tumours: Hypoenhancement on arterial phase computed tomography predicts biological aggressiveness. *HPB (Oxford).* 2014;16:304-311.

24. Jeon SK, Lee JM, Joo I, et al. Nonhypervascular pancreatic neuroendocrine tumors: Differential diagnosis from pancreatic ductal adenocarcinomas at MR imaging-retrospective cross-sectional study. *Radiology.* 2017;284:77-87.

FIGURE LEGENDS

Figure 1.

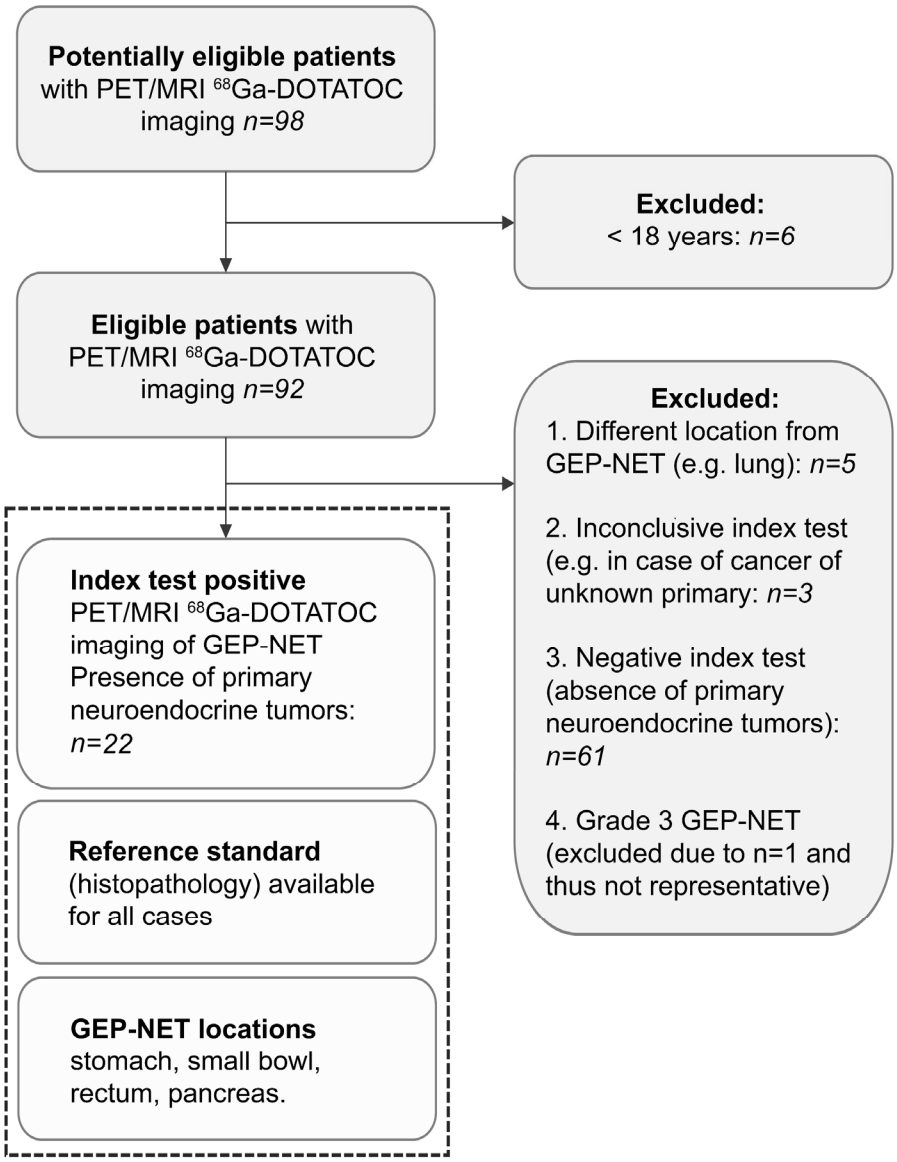

Study flow chart. *Abbreviation:* GEP-NET: Gastroendopancreatic neuroendocrine tumor.

Figure 2.

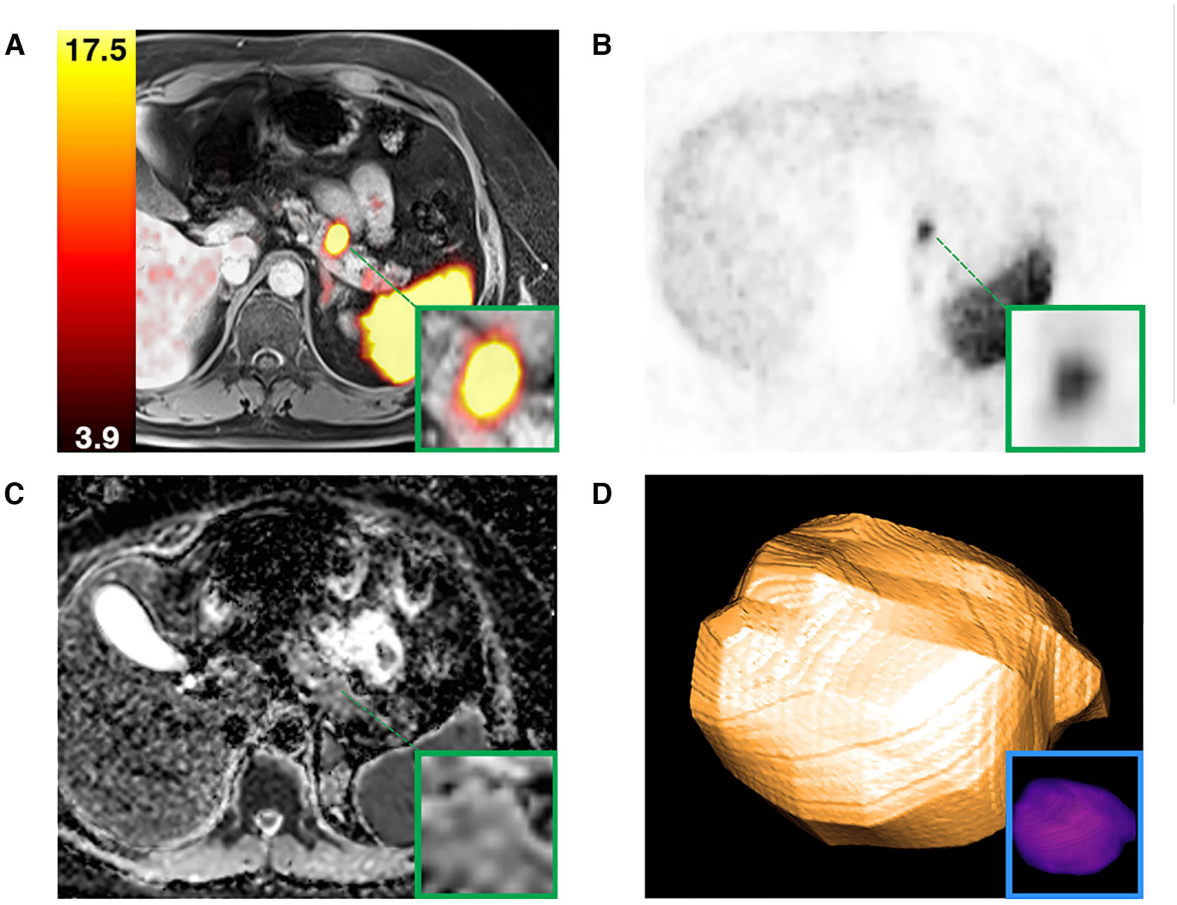

Example of 3D volume of interest (VOI) lesion analysis in a 50-year old patient with a grade 1 pancreas NET (SUV_{mean} of 15 and an ADC_{min} of 900 mm^2/s, combined ratio SUV_{mean}/ADC_{min}: 0.02). (A) fusion of postcontrast T1 VIBE with ^{68}Ga-DOTATOC PET, (B) ^{68}Ga-DOTATOC PET, (C) ADC map and (D) 3D lesion model. *Abbreviations:* NET: Neuroendocrine tumor; ADC: Apparent diffusion coefficient.

Figure 3.

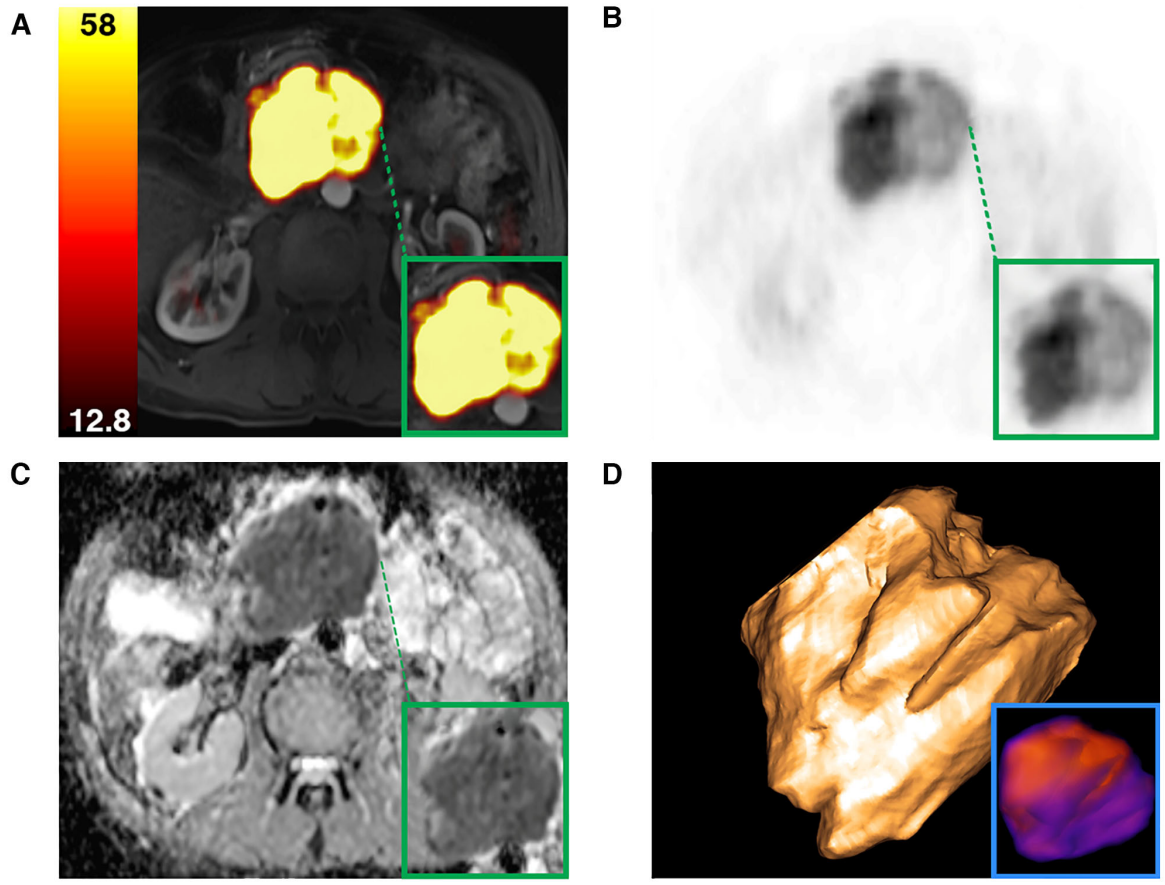

Example of 3D volume of interest (VOI) lesion analysis in a 64-year old patient with a grade 2 pancreas NET (SUV_{mean} of 45 and an ADC_{min} of 490 mm^2/s, combined ratio SUV_{mean}/ADC_{min}: 0.09). (A) fusion of postcontrast T1 VIBE with ^{68}Ga-DOTATOC PET, (B) ^{68}Ga-DOTATOC PET, (C) ADC map and (D) 3D lesion model. *Abbreviations:* NET: Neuroendocrine tumor; ADC: Apparent diffusion coefficient.

Figure 4.

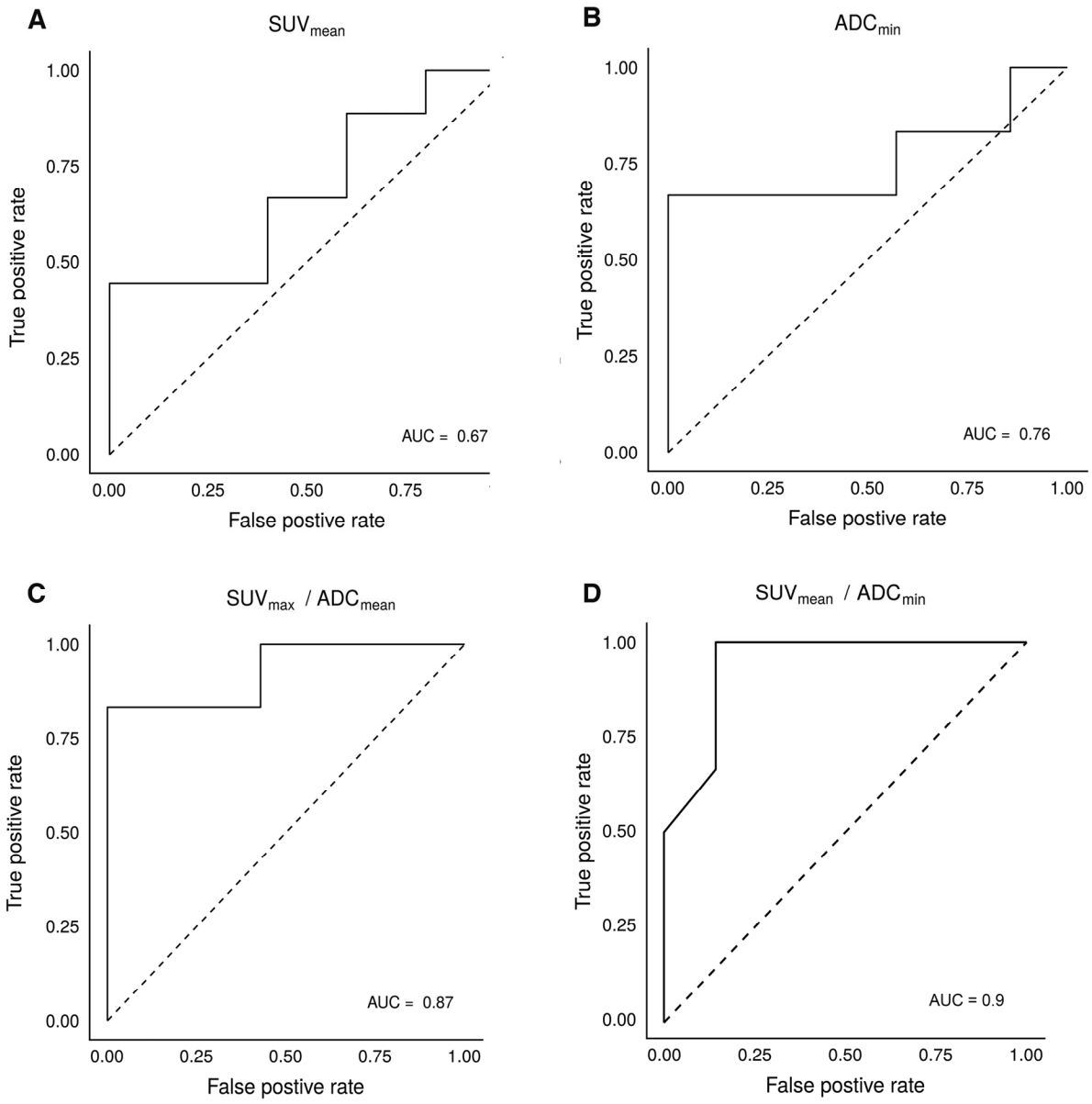

Receiver operating characteristic (ROC) curves from ^{68}Ga-DOTATOC PET and MRI apparent diffusion coefficient (ADC) parameters. SUV_{mean} (A) demonstrates poor to moderate discriminative test performance, while ADC_{min} shows a fair discriminative ability. Out of the combined ratios (C, D) and parameters, SUV_{mean}/ADC_{min} (D) demonstrates the best discriminative test performance, with an AUC of 0.90, and a sensitivity of 86% and specificity of 100%. *Abbreviation:* AUC: Area Under the Curve.

TABLES

Table 1. Patient- and tumor-related characteristics.

Characteristics	**Mean ±SD (range) | *Number (%)***
Age (years)	61 (43-81 years)
Sex	
Male	15 (68.2 %)
Female	7 (31.8 %)
Histologic tumor grade (24 lesions)	
Grade 1	12 (50 %)
Grade 2	12 (50 %)
Tumor location	
Stomach	1 (4.2 %)
Small bowel	9 (37.5 %)
Rectum	1 (4.2 %)
Pancreas	13 (54.2 %)
Presence of metastases	20 (80.0 %)

Table 2. MRI sequence parameters.

Sequence	Orientation	Bandwidth (Hz/Px)	TR/TE (ms)	Matrix	FOV (mm)	Voxel size (mm^3)	TA (s)
T2w HASTE	Axial	710	1,400/95	320	400	1.3x1.3x5.0	68
T2w TIRM	Coronal	300	4,390/53	256	450	1.8x1.8x4.0	142
T1w fs VIBE	Axial	450	3,9/1,86	320	400	1.3x1.3x3.0	17
T2w fs TSE	Axial	243	2,200/100	448	400	0.9x0.9x5.0	230
EPI DWI	Axial	2232	5,600/55	134	380	1.4x1.4x5.0	204
T1w fs VIBE (dynamic)	Axial	450	3.95/1.92	320	360	1.1x1.1x3.0	17 (per phase)
T1w fs STARVIBE	Axial	870	3.05/1.44	320	380	12.x1.2x1.2	278

Table 3. Comparison of Imaging Parameters Between Different World Health Organization Grade GEP-NET.

Imaging parameter	Grade 1 (n=12) ±SD (range)	Grade 2 (n=12) ±SD (range)
Diameter (mm)	19.7±9.6 (12.0-95.0)	40.7±30.4 (11.0-40.0)
Total functional tumor volume (cm^3)	6.4±9.9 (1.2-34.2)	70.6±112.2 (1.5-351.1)
Ki-67 proliferation index (%)	1.6±0.6 (0.9-2.0)	5.3±2.6 (2.3-10)
TBR	6.6±1.9 (3.1-10.1)	12.7±9.3 (3.9-33.2)
SUV_{mean}	14.7±7.0 (4.0-23.2)	23.1±12.3 (8.0-45.0)
SUV_{max}	34.9 ± 16.9 (14.5-62.5)	42.3 ± 26.6 (14.8-89.5)
ADC_{mean} ($*10^{-3}$ mm^2/s)	1.24 ±0.18 (1.05-1.49)	0.96±0.26 (0.50-1.22)
ADC_{min} ($*10^{-3}$ mm^2/s)	0.67 ±0.14 (0.51-0.87)	0.49±0.24 (0.23-0.85)
Enhancement ratio	1.2±0.8 (0.6-2.9)	1.0±0.4 (0.4 to 1.6)

SUPPLEMENTAL DATA

Supplemental Figure 1.

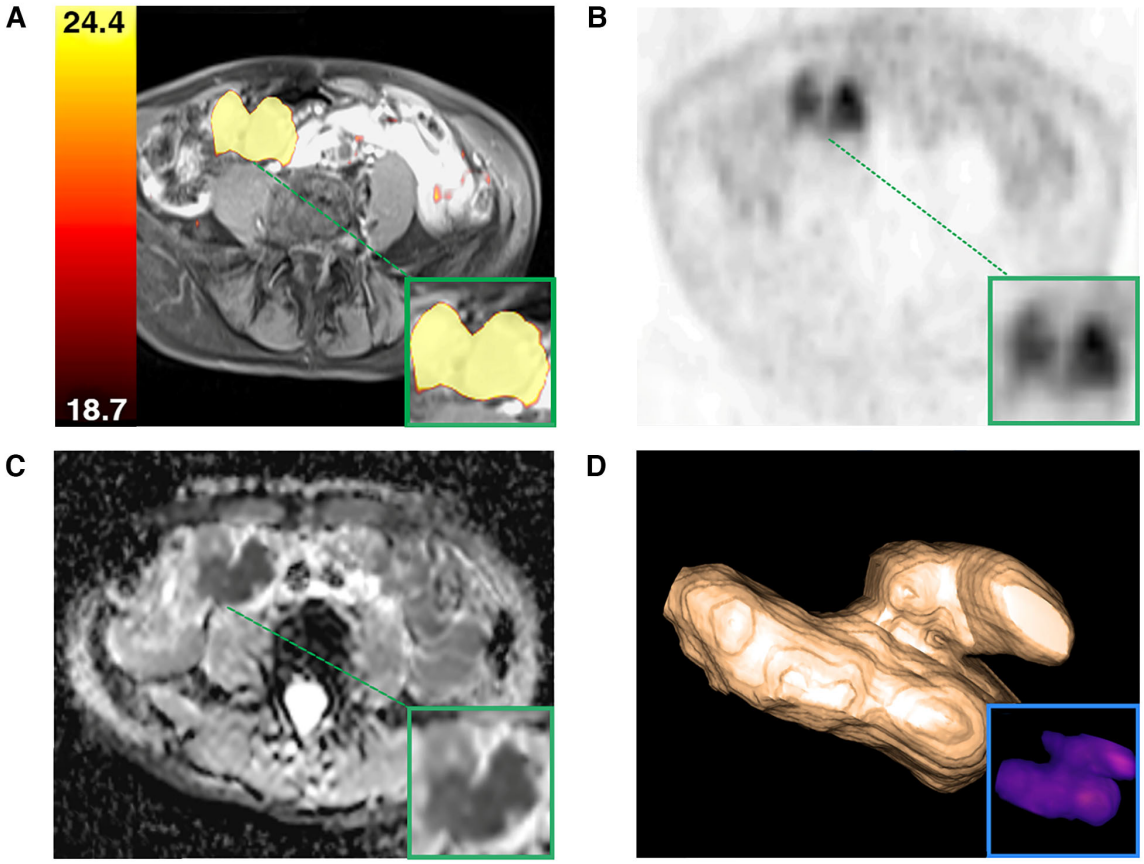

Example of 3D volume of interest (VOI) lesion analysis in a 76-year old patient with a grade 2 ileum NET (SUV_{mean} of 13 and an ADC_{min} of 360 mm^2/s, combined ratio SUV_{mean}/ADC_{min}: 0.04). (A) fusion of postcontrast T1 VIBE with ^{68}Ga-DOTATOC PET, (B) ^{68}Ga-DOTATOC PET, (C) ADC map and (D) 3D lesion model. *Abbreviations:* NET: Neuroendocrine tumor; ADC: Apparent diffusion coefficient.

Supplemental Figure 2.

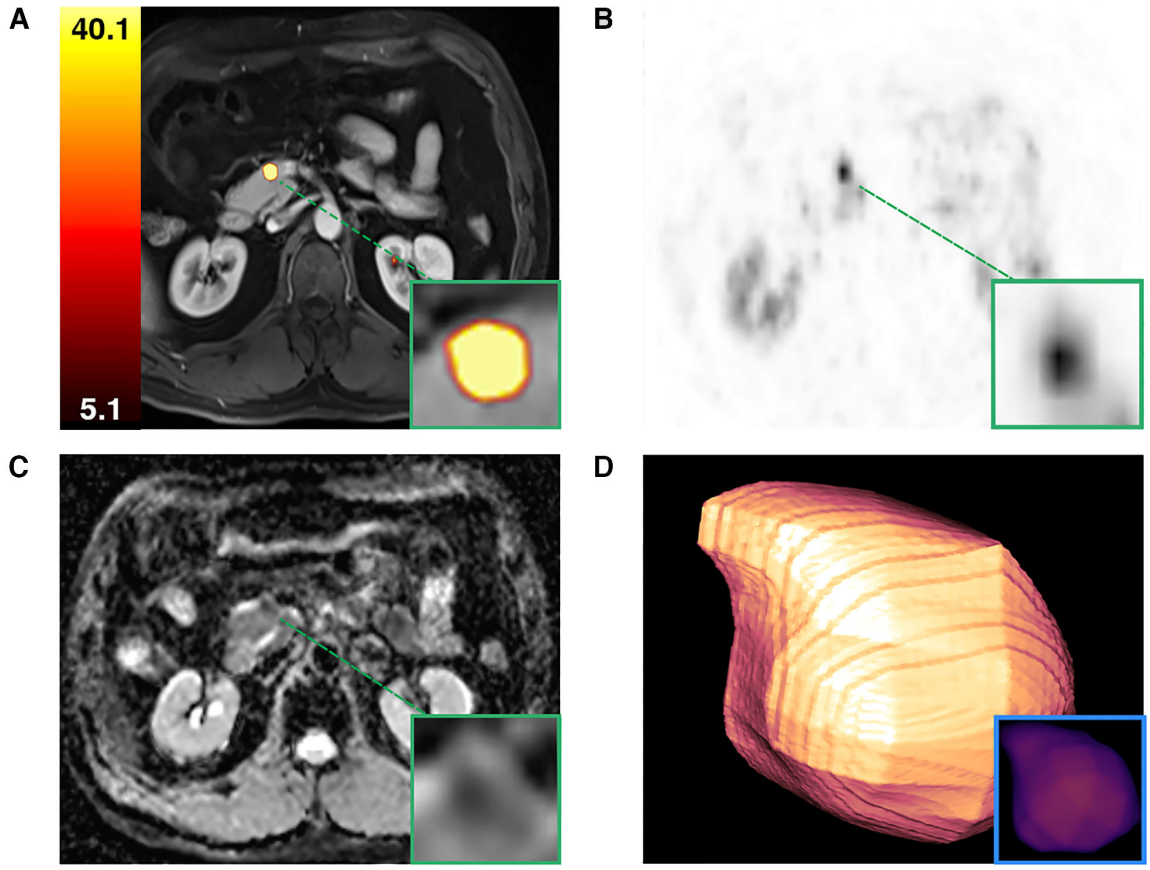

Example of 3D volume of interest (VOI) lesion analysis in a 53-year old patient with a grade 2 pancreas NET (SUV_{mean} of 32 and an ADC_{min} of 824 mm^2/s, combined ratio SUV_{mean}/ADC_{min}: 0.04). (A) fusion of postcontrast T1 VIBE with ^{68}Ga-DOTATOC PET, (B) ^{68}Ga-DOTATOC PET, (C) ADC map and (D) 3D lesion model. *Abbreviations:* NET: Neuroendocrine tumor; ADC: Apparent diffusion coefficient.

Supplemental Figure 3.

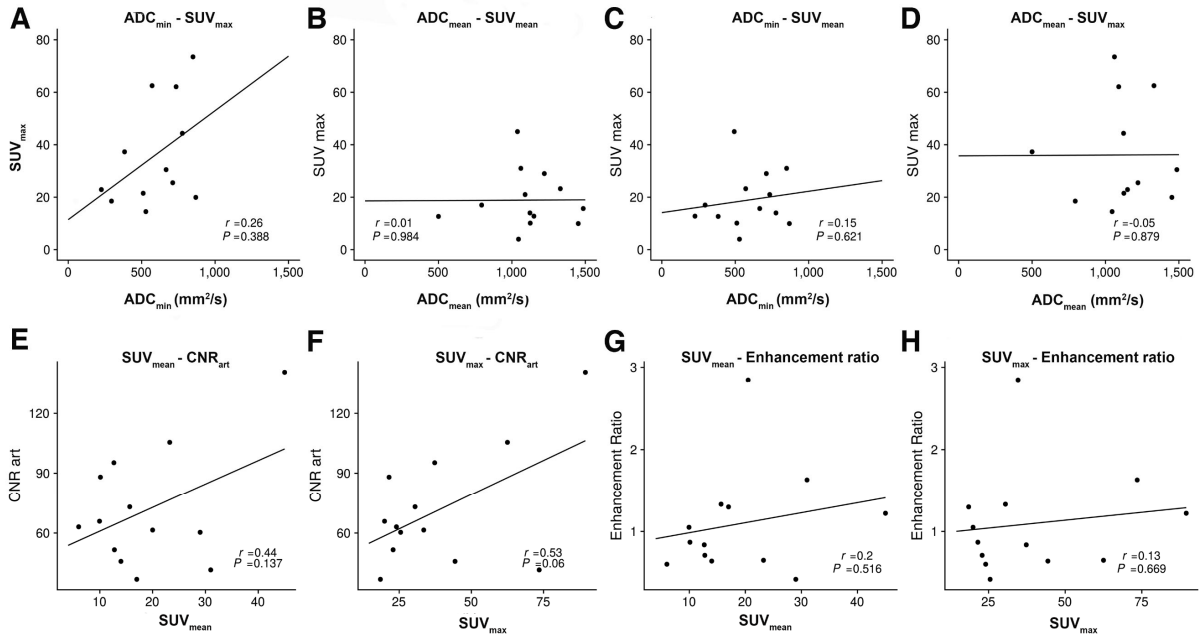

Scatter plots of correlation between tumor apparent diffusion coefficient (ADC) and standardized uptake value (SUV) values and between the SUV and arterial enhancement parameters (contrast-to-noise-ratio (CNR) and enhancement ratio (ER)) as determined on ^{68}Ga-DOTATOC PET/MRI from 24 GEP-NET in 22 patients. For each scatterplot, the best-fit line is shown as the solid line. (A), ADC_{min} versus SUV_{max}; (B), ADC_{mean} versus SUV_{mean}; (C), ADC_{min} versus SUV_{mean}; (D), ADC_{mean} versus SUV_{max}; (E) SUV_{mean} versus $CNR_{art,}$ (F) SUV_{max} versus CNR_{art}, (G) SUV_{mean} versus enhancement ratio, and (H) SUV_{max} versus enhancement ratio. *Abbreviation:* CNR_{art}: arterial contrast-to-noise ratio.